TI-6AL-4V ADDITIVE MANUFACTURING MECHANICAL PROPERTIES AS INDICATION TO MEASURE OF QUALITY

Carmel Matias[1], Dr. Alex Diskin[2], Dr. Oz Golan[3], Garkun Andrey[4] and Evgeny Strokin[4]

[1] Fatigue and Damage Tolerance Dept., Engineering & Development Center, Aviation Group, Israel Aerospace Industries (IAI), 70100 Ben-Gurion International Airport, Israel, cmatias@iai.co.il
[2] Material Engineering & Technology Development Dept., Aviation Group, Israel Aerospace Industries (IAI), 70100 Ben-Gurion International Airport, Israel
[3] Afeka Center for Materials and Processes Engineering, Afeka- Tel-Aviv Academic College of Engineering, Mivtza Kadesh St. 38, 6998812 Tel-Aviv, Israel
[4] The Israel Institute of Metals, the Technion, 32000 Haifa, Israel

Abstract: Additive Manufacturing (AM) technology, has not yet been adopted by the airframe industry to produce primary load carry structural items. This is mainly due to lack of generic economic quality control methods to detect manufacturing defects that compromise fatigue strength. This study presents an allowed defects characterization approach, derived from testing results, to provide data for quality control acceptance criteria. Elongation and fatigue (crack-initiation) test results strongly related to AM production quality (per defects variety), whereas, crack-growth results were not affected by the studied defects (as all specimens were stress relieved). Further studies are needed to provide defects characterization to derive detailed quality control rejection criteria.

Keywords: AM, 3D-Printing defects, Ti-6AL-4V PBF, SLM, Fatigue strength

INTRODUCTION

AM technology (also called 3D-Printing) is facing implementation challenges in the aviation industry to produce metal airframe load carry items (Principal Structural Element – PSE [1]). AM technology is not yet considered mature for PSE's serial production, mainly due to lack of generic economic quality control methods, to detect manufacturing defects that compromise fatigue strength. Well-established and extensively used Non-Destructive Inspections (NDI) techniques such as: Ultra-sonic, Eddy-current, Liquid-penetrant, etc., cannot detect the AM technology inherent defects, of which triggers fatigue failures [2]. These NDI techniques are basically independent of specific product manufacture procedure (generic) and are economic. Present AM defects detection requires either "tailor-made" techniques or Computer-Tomography (CT) technology, which are not practical for airframe industry serial production.

This study done for Ti-6AL-4V Powder Bed Fusion (PBF), Selective Laser Melting (SLM) technology, presents an approach of allowed defects characterization to be used for quality control criteria, based on experiments accompanied by Micro-CT inspections and SEM/Fractographic failure analyses. The study examined effects on mechanical properties for AM defect type of: pores (local voids), lack of fusion

surfaces and inclusions (contaminations), for relations of defect size per its distance to surface. Another AM defect type is residual stress fields, that are known to have a strong impact on fatigue crack growth [3]. This study did not include residual stresses since all specimens had done Heat Treatment procedures that relieved internal stresses

THE SPECIMENS TESTED AND THE EXPERIMENTAL CAMPAIGN

The following three mechanical tests were done via the following specimens:

- Quasi-Static Test per ASTM E8 [4]; Test specimen: 12 mm diameter round bar.
- Fatigue (crack initiation) Test per ASTM E466-15 [5], R=0.1, Round Bar specimen with continuous radius between Ends (Neck=5mm dia., Ends=10mm dia.), Kt=1.0.
- Crack Growth Test per ASTM E647−15 [6], R=0.1, Compact Tension C(T) Specimen having: Width=30 mm, Thickness=5 mm, Artificial notch length=5 mm.

In order to examine the AM Defects in the context of the mechanical testing results, the quality of the specimens was studied by Metallurgical and Micro Computer Tomography (Micro-CT) inspections, and failure analyses were conducted (Fractographic via SEM).

This study was done for Ti-6Al-4V powder processed by Selective Laser Melting (SLM) via Powder Bed Fusion (PBF) AM technology, using ALM EOS M290 Machine (using Laser-Power of 340W producing Print-Layer-Thickness of 60µm). All specimens were printed with printing layer orientation perpendicular to specimen's loading direction (the weakest orientation), and machine processed to produce the required dimensions for each test (per relevant ASTM Specification), including N6 (32µin) surface roughness quality level.

Eight distinct specimen type were produced providing different qualities expressed by defects variety to examine their effects of on mechanical properties. The distinct specimen types were configured by:

- Tour different AM parameters sets (the print qualities are per [7]), via different printing Trays:
  - Tray #1 – All printing parameters were the EOS recommendation → Good quality.
  - Tray #2 – One parameter only: "Stripe-Width", was modified to double the recommendation (all other parameters were per the EOS recommendation) → Best / improved quality.
  - Tray #3 – One parameter only: the "Stripes-Distance", was modified to double the recommendation (all other parameters were per the EOS recommendation) → Poor-quality.
  - Tray #4 – One parameter only: the "Beam-Power", was modified to half the recommendation (all other parameters were per the EOS recommendation) → The worst quality.
- Two different thermal treatments procedures applied to each Printing-Parameters-Set. Half the number of specimens produced for each one of the four different AM Printing-Parameters-Set, were thermal Post-Processed by either one of the following two procedures:
  - Heat Treatment (HT) of 800ºC for two hours at Argon atmosphere (no pressure applied).
  - Hot Isostatic Pressing (HIP) per ASTM F3001 (heat treatment under pressure condition).

Figure 1 presents graphics for the laser beam travel printing parameters of Stripe-Width and Stripe-Distance. Figure 2 presents the four different parameter sets printed specimens, and tensile machines used for the tests, in the Laboratory.

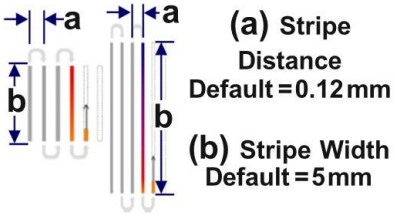

Figure 1: "Stripe-Width" & "Stripes-Distance" printing parameters.

Figure 2: AM tested specimens, for the four print parameters sets and testing machines.

TESTING RESULTS AND DISCUSSION

The Quasi-Static Tests

Table 1 presents the number of specimens tested per distinct specimen type, the average results per each distinct type, individual results per specimen and the ASTM requirements. All the test results that did not met the minimum ASTM requirements, are marked on Table 1 (by red rectangles).

Test results for all the Good-printing-quality specimens (printed via trays #1 & #2), had well met ASTM requirements (for with and without HIP treatment). Note that the improved quality of tray #2 printing parameters had shown significant high Elongation results. Test results for all the Worst-printing-quality specimens (printing tray #4) did not meet the ASTM requirements (for with and without HIP treatment were far below requirements, i.e. HIP did not "repair"). The Poor-printing-quality specimens (printing tray #3) had shown mixed test results that provided meaningful information to the parameters for quality investigation. The tray #3 specimens had presented the following Elongation results, regarding the HIP treatment application:

- The three specimens that did not do HIP treatment had shown Elongation results that did not meet the ASTM requirement, and were far below requirement.
- Among the five specimens that did the HIP treatment, for two of them the Elongation result did not meet ASTM requirements (being far below requirements), but, for the other three specimens the Elongation results met very well the requirements (far above requirement). These test results suggest that the HIP procedure had managed to "repair" defects (effecting Elongation) such as Pores (Local Voids), that the pressure application could "close" (Pore size diameter reduction to below 50 μm up to below detection limit of 22 μm, depending on initial As-Built Pore size [10]), but did not managed to "repair" other defects such as Lack of Fusion Surfaces and Inclusions (Contaminations), as HIP procedure cannot create "complementary" Fusion or eliminate Contaminations. Furthermore, as each specimen was individually marked, having its own unique identification and being followed since its specific location in the printing tray, it had been shown that low Elongation results were related to tray location near Argon-Gas Outlet/Inlet, suspicious for potential Inclusion Defects zone, as presented in Fig. 4 for the specimen's location in the printing tray per test results (which will be further discussed also at the next section).

The Fatigue (Crack Initiation) & Fatigue-Crack-Growth Tests

Fatigue (crack initiation) and Crack-Growth tests were done on Round Bars (Kt=1) and C(T) Specimens, respectively, for the specified above 8 distinct specimen type. The number of specimens tested per each distinct specimen type, for the fatigue and for the crack-growth tests, are presented in Table 2 and Table 3, respectively.

Table 1: Results for the Quasi-Static Test (per Specimen and average).

Tray #	Thermal Treatment (Number of Specimens)	Modulus [Gpa]	Tensile Strength (UTS) [Mpa]	Yield Strength $R_{p0.2}$ [Mpa]	Elong. ε_f [%]
1	Stress relief HT (3)	118	1,113	1,070	13.3
	HIP (5)	118	1,011	933	11.5
2	Stress relief HT (3)	118	1,103	1,053	16.5
	HIP (5)	118	1,007	918	17.2
3	Stress relief HT (3)	105	955	910	2.8
	HIP (5)	114	953	886	10.6
4	Stress relief HT (3)	95	855	803	0.8
	HIP (5)	95	805	743	0.9
ASTM F3302-18 Requirements		110	895 Min.	825 Min.	10 Min.

Tray #1 Specimens

Specimen ID		Yield Stress 0.2p, MPa	UTS, MPa	Elongation (l0=25mm), %
P1m-03	Stress Relief HT	1071	1111	13.5
P1m-05		1070	1114	13.2
P1m-07		1068	1115	13.3
av		1069.67	1113.33	13.33
std		1.25	1.70	0.12
P1m-02	HIP	934	1012	11
P1m-04		922	1005	12
P1m-06		936	1013	12
P1m-08		931	1011	11.7
P1m-10		940	1013	10.7
av		932.60	1010.80	11.48
std		3.99	1.22	0.56

Tray #2 Specimens

Specimen ID		Yield Stress 0.2p, MPa	UTS, MPa	Elongation (l0=25mm), %
P2m-03	Stress Relief HT	1050	1102	16.7
P2m-05		1056	1104	16.5
P2m-07		1053	1102	16.3
av		1053.00	1102.67	16.50
std		2.45	0.94	0.16
P2m-02	HIP	916	1004	17.1
P2m-04		918	1006	17.3
P2m-06		920	1010	17.3
P2m-08		920	1011	17
P2m-10		917	1004	17.2
av		918.20	1007.00	17.18
std		1.47	3.16	0.12

Tray #3 Specimens

Specimen ID		Yield Stress 0.2p, MPa	UTS, MPa	Elongation (l0=25mm), %
P3m-03	Stress Relief HT	898	909	0.5
P3m-05		920	978	4.0
P3m-07		912	978	4.0
av		910.00	955.00	2.83
std		9.09	32.53	1.65
P3m-02	HIP	895	960	3
P3m-04		894	983	16.7
P3m-06		899	986	16.5
P3m-08		848	853	0.5
P3m-10		895	981	16.3
av		886.20	952.60	10.60
std		23.32	61.87	7.50

Tray #4 Specimens

Specimen ID		Yield Stress 0.2p, MPa	UTS, MPa	Elongation (l0=25mm), %
P4m-03	Stress Relief HT	768	809	0.5
P4m-05		818	876	1.5
P4m-07		824	881	1.5
av		803.33	855.33	1.17
std		25.10	32.83	0.47
P4m-02	HIP	734	803	1.8
P4m-04		760	839	2.2
P4m-06		766	795	0.5
P4m-08		746	806	1.1
P4m-10		710	782	1.5
av		743.20	805.00	1.42
std		23.21	11.17	0.45

Table 2: Number of Specimens Fatigue (crack initiation) Tested par distinct Specimen type

Printing Parameters / Tray #	Number of Specimens Tested: Stress Relieved HT (as specified above)	Number of Specimens Tested: HIP per ASTM F3001
Tray #1	10	10
Tray #2	9	9
Tray #3	9	10
Tray #4	9	10

Table 3: Number of Specimens Crack-Growth Tested par distinct Specimen type

Printing Parameters / Tray #	Number of Specimens Tested: Stress Relieved HT (as specified above)	Number of Specimens Tested: HIP per ASTM F3001
Tray #1	5	2
Tray #2	5	2
Tray #3	5	2
Tray #4	4	1

Figure 3 shows the Fatigue test results for number of cycles to failure per Max. Cyclic Loading Stress (R=0.1, Kt=1), presented by the diamond-dots (via 8 different color-shades per the 8 distinct specimen types, specified as "P1" to "P4" designating each of the four printing trays followed by "AB" for the heat-treatment without pressure, or "HIP" for the HIP procedure treatment), in comparison to:

(a) Results of a previous testing program conducted via the "AATiD" Consortium [7], presented by brown color-shade stripes accompanied with "Best Fit" curve (black color-shade curve) and "B Value Stress" curve (red color-shade curve).
(b) MMPDS Handbook Data [8], presented by the light-blue color-shade curve.

Figure 3 also presents Weibull statistical analysis results for each distinct specimen type (per its 7 to 10 individual specimen results), in the terms of "Characteristic-Life" and Variance level (shape parameter). The statistical analysis accounted for failures and non-failures, per the number of cycles that caused specimen failure, and number of cycles that did not cause specimen failure (of which specimen either didn't fail, or failed in the Tensile-Machine-Grips). The total number of specimens (failed + not-failed) over the number of specimens that were accounted as not-failed, are denoted as: "(n/s)". Figure 3 also presents 8 oval shapes in the different color-shades as are for the 8 distinct specimen types, to graphically present the spread (variance) of the Fatigue results, for each of the 8 distinct specimen type.

$8X10^6$ cycles and up are the required Fatigue life results. Specimens achieving lower fatigue life suggested defects to be studied by SEM/Fractographic failure analyses. The different printing qualities and the HIP treatment provided extensive differentiation in the defect types and dimensions (size and distance to surface) to be studied, as can be seen by the extensive variety in the fatigue life results achieved. Table 4 shows observations for results comparison to previous AATiD [7] testing. Both trays #1 and #2 printing qualities, enabled the HIP procedure to effectively increase fatigue life and dramatically decrease life results spread by introducing dominant defect type of Pores having "repairable" sizes (per [10]) for the HIP procedure. The improved tray #2 printing quality is expressed by achieving the required Fatigue life as the characteristic result, for even the non-HIP specimens. The extremely poor tray #4 printing quality is expressed by achieving extremely low fatigue results for HIP & non-HIP specimens. Tray #3 print presented extensive defect type and dimensions variety, such that non-HIP specimens achieved very low fatigue results with low variance level, and HIP application had dramatically increased life results spread by different "repair" levels for the different defect type and dimensions. This tray #3 print quality provided lots of information to the failure analyses study.

Fig. 4 presents the Fatigue & Quasi-Static specimens with their marked identification-code, as they were placed at the printing tray (#3) and the chamber's Argon-Gas Inlet/Outlet orientation. Fig. 4 also presents the HIP specimens Fatigue & Static test results for being above or under specified criteria (as specified in the Figure). It is seen that tray locations near Argon-Gas Outlet/Inlet were related to low fatigue life. These Outlet/Inlet locations may be prone to higher Inclusion-density ambience, inducing Inclusion-Defects effecting on the test results (as such indications were found in the failure analyses done).

Table 4: Crack initiation test results observations compare to previous testing of AATiD [7] program

	Characteristic-Life	Variance Level
Tray #2 Printing		
HIP –	Corresponds well to "AATiD" results	Low
NO-HIP(*) –	Corresponds well to "AATiD" results	Very High
Tray #1 Printing		
HIP –	Corresponds well to "AATiD" results	Low
NO-HIP(*) –	~ 0.5 Factor of "AATiD" results	Very High
Tray #3 Printing		
HIP –	~ 0.3 Factor of "AATiD" results	Very High
NO-HIP(*) –	Extremely low	Low
Tray #4 Printing		
HIP –	Most extremely low	Extremely Low
NO-HIP(*) –	Most extremely low	Low
(*) Stress Relieve Heat Treatment of 2 hours at 800ºC with no pressure applied.		

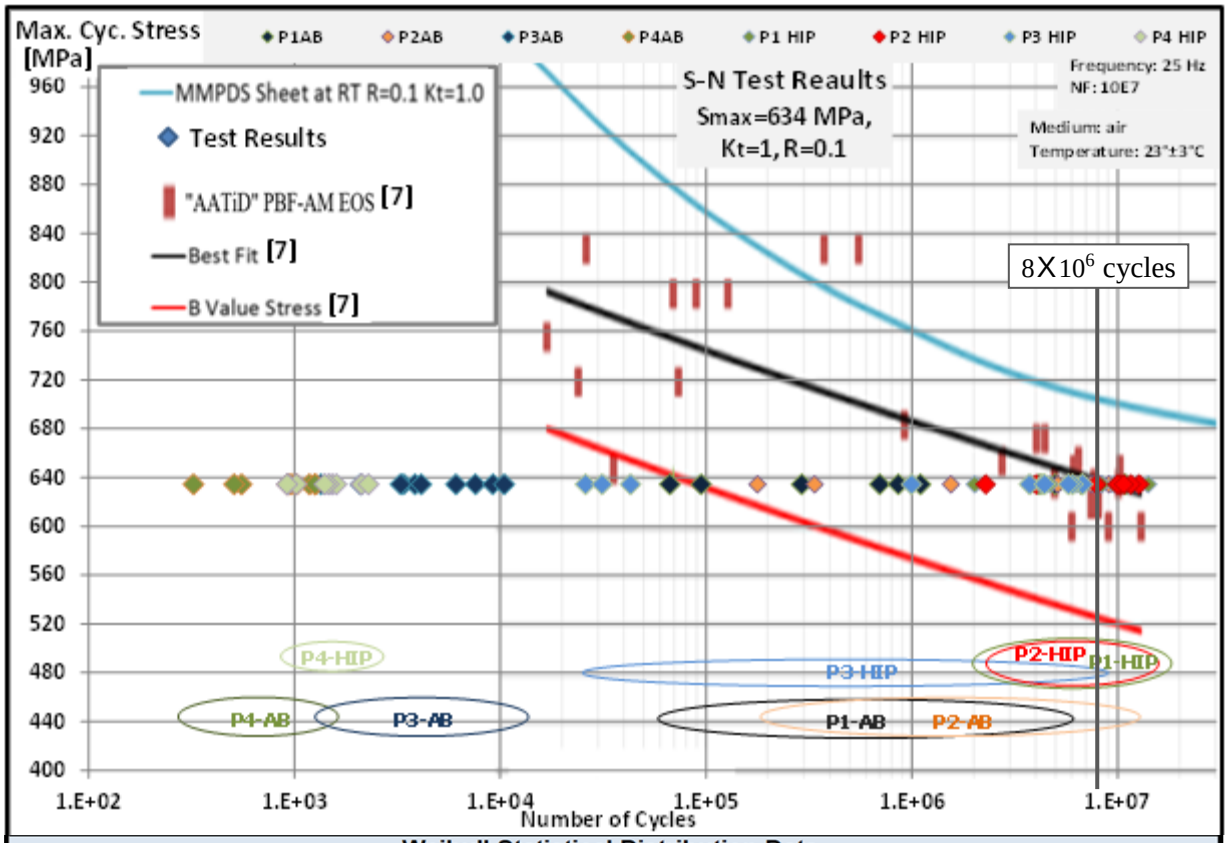

Weibull Statistical Distribution Data

AB			HIP		
Tray#	Shape Parameter/Variance (n/s)	Characteristic Life	Tray#	Shape Parameter/Variance (n/s)	Characteristic Life
P1	0.787 (8/2)	5,194,789 Cycles	P1	3.067 (10/3)	10,417,260 Cycles
P2	1.485 (7/3)	9,455,652 Cycles	P2	2.502 (9/4)	12,190,150 Cycles
P3	1.630 (9/0)	6,101 Cycles	P3	0.515 (10/0)	2,610,585 Cycles
P4	2.380 (9/0)	1,014 Cycles	P4	3.448 (10/0)	1,699 Cycles

Figure 3: Fatigue (crack initiation) Test Results for all 8 Specimen Types

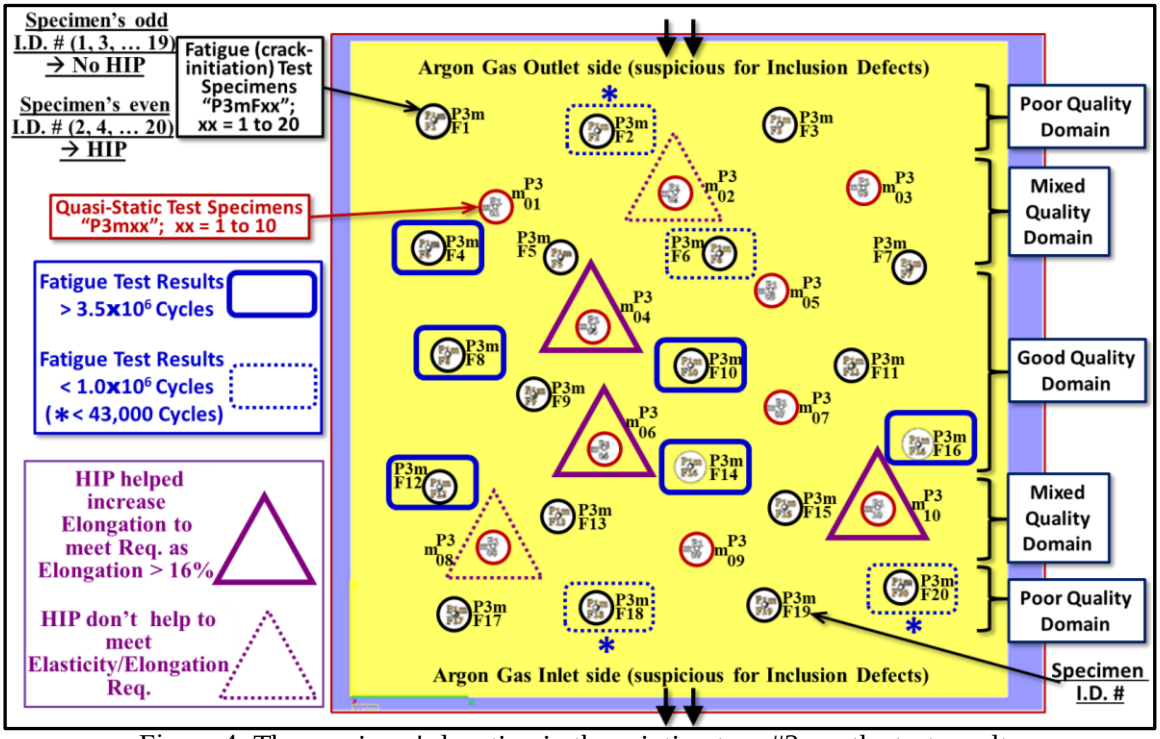

Figure 4: The specimen's location in the printing tray #3 per the test results

Fig. 5 presents the Crack-Growth test results in terms of crack growth rate (Inches of crack length per number of applied loading cycles, da/dN) vs. Stress Intensity range (in units of KSI X √Inches, ΔK), for HIP and non-HIP specimens (via different dots) per each printing tray (#1 to #4). The test results are presented in comparison to NASGRO computer program da/dN vs. ΔK data [9] (that is well accepted and extensively used in the airframe industry) for Ti-6AL-4V Forges & Plates (red color-shade curves). It can be seen that the crack growth test results for all printing tray specimens (HIP & non-HIP) correlate well to the NASGRO computer program da/dN vs. ΔK data, to all the ΔK range tested (note that two printing tray #4 specimens had presented some higher da/dN's for relatively high ΔK's, compare to the NASGRO computer program data). Neither of the four printing parameters sets (per the four printing trays) nor the two HT (HIP & non-HIP), had any significant effect on crack growth rates compare to the NASGRO da/dN vs. ΔK data. This is explained by the fact that both HIP & non-HIP HT had effectively eliminated residual stresses, of which, residual stress strongly impacts fatigue crack growth, whereas defect type of Pores, Lack-of-Fusion Surfaces (and Inclusions) does not influence crack growth ([3]).

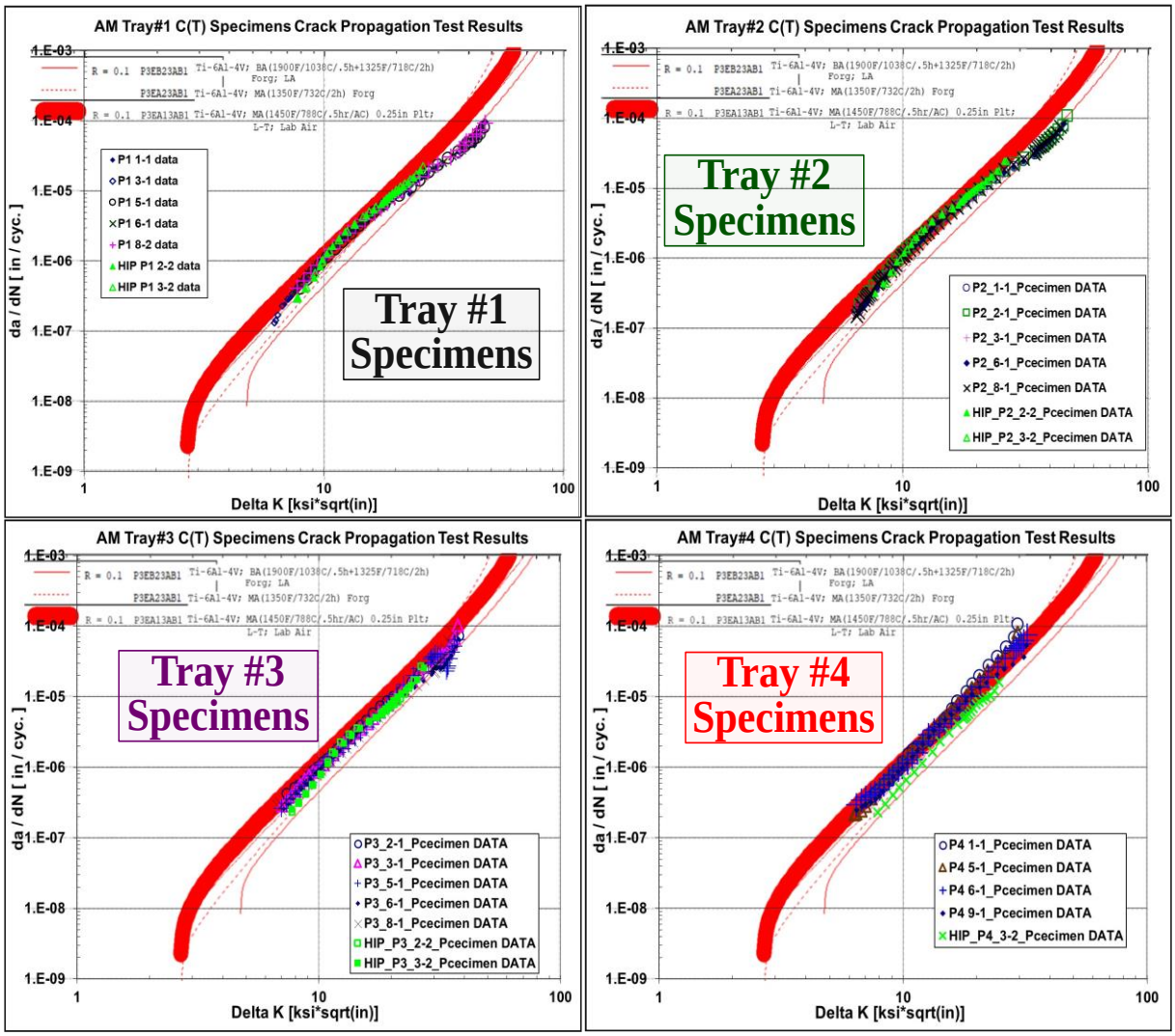

Figure 5: Crack Growth Test Results for Tray's #1 to #4 Specimens (No-HIP & HIP)

AM DEFECT FINDINGS EVALUATED BY THE MICRO-CT INSPECTIONS & SEM/FRACTOGRAPHIC FAILURE ANALYSES

Micro-CT inspections done (prior to testing) for the eight distinct specimen type, had presented findings of defects count per sizes and their locations (clusters, distances, etc.), and the Relative-Density finding (Note: Relative-Density definition is the ratio of the density of an Additive Manufactured Ti-6AL-4V to the density of Ti-6AL-4V made from Forges/Plates). SEM/Fractographic failure analyses were done for the specimens that had completed the fatigue (crack initiation) tests, to reveal the cracking source for its specific type, size and its location-distance to surface.

Fig. 6 presents Micro-CT inspection results example, for printing tray #1 specimen (having HT with no pressure, i.e. no HIP). This Fig. presents: defect size per count histogram, Relative-Density finding of 0.00, and zoom-in on a specific fatigue-critical near surface pore defect having 100 µm for both is size and its distance to surface. Such defect finding present an example for good printing quality (for tray #1 specimens having accepted Relative-Density and low defect size per count), that still is not expected to meet fatigue requirements due to potential early fatigue cracking out of this "zoom-in" presented defect.

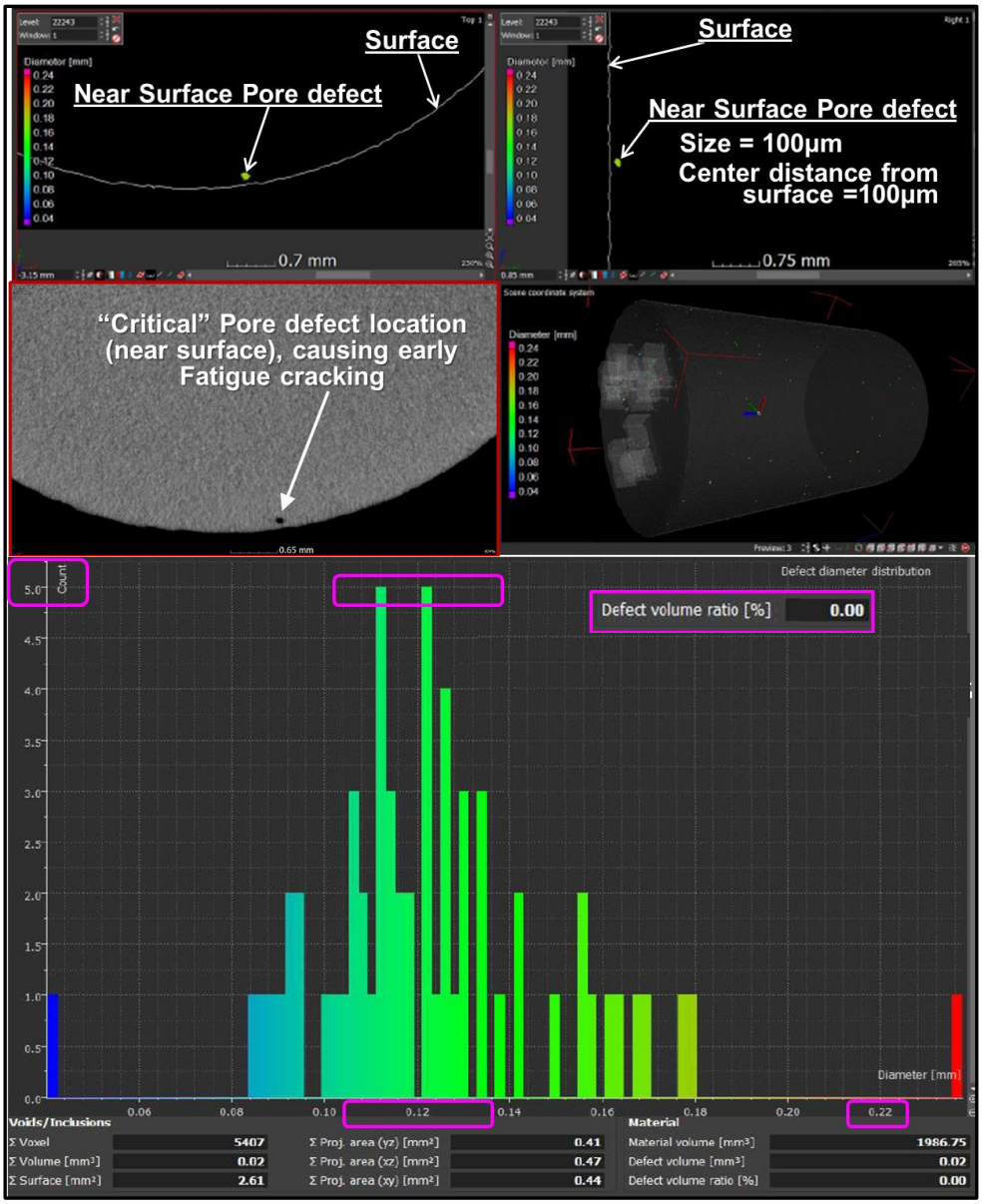

Figure 6: Tray #1 Specimen (No-HIP) Micro-CT inspection results (defect size per count & location)

Fig. 7 presents Micro-CT inspection results example, for printing tray #3 specimen (having HT with no pressure, i.e. no HIP) showing high defect count and large defect sizes. The Relative-Density finding is 97.94% (i.e. 2.06% Defect-Density). These defects findings present an example for poor printing quality that is certainly not expected to meet fatigue requirements.

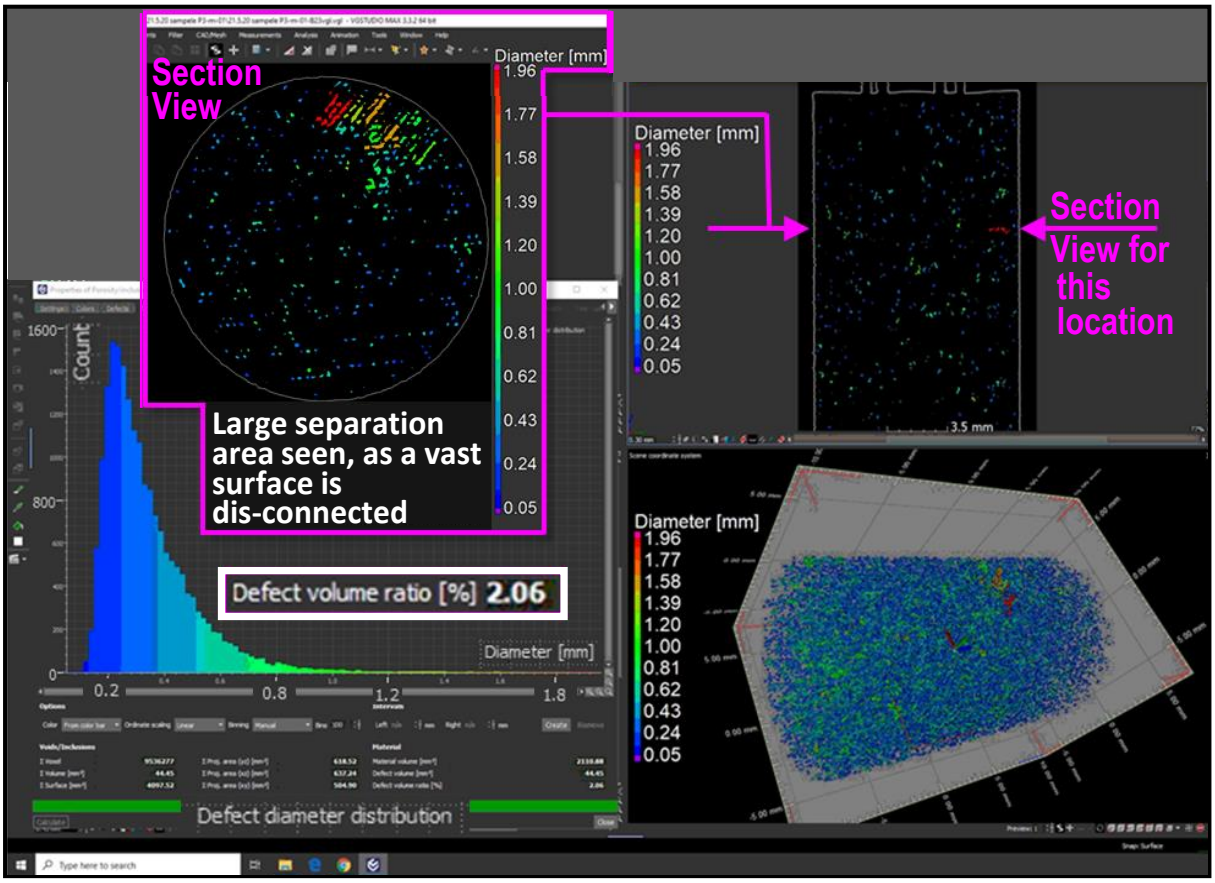

Figure 7: Tray #3 Specimen (No-HIP) Micro-CT inspection results (defect size per count & location)

Fig. 8 presents SEM/Fractographic failure analysis results example for tray #3 specimen (HIP), showing lots of internal Lack-of-Fusion-Surface defects, of which some are being located very near surface. That specific specimen (I.D. P3-m-F2) had failed early into the fatigue test, at only 42,887 cycles. The cracking had initiated from these defects. Since that specific specimen had undergone the HIP procedure, it's understood that the HIP procedure did not "repair" these defects (and the specimen had remained having porous structure even after HIP, in inner locations and near surface).

Fig. 9 presents SEM/Fractographic failure analysis results example for tray #2 specimen (No-HIP), that happened to have an internal defect having a size of ~90µm, located at 850-to-900µm distance from the surface. This detect was the source for fatigue crack initiation. The fatigue failure result for this specimen (I.D. P2-m-F17) was high, as required for the cyclic loading applied, of 9,758,414 cycles to failure. The SEM/Fractographic failure analysis revealed a good printing quality, except for that defect of which was identified as an inclusion/contamination defect (that prevented solidification joining around its periphery). This fatigue result shows that such a defect of having its size and distance from surface, is not critical-for-fatigue strength, and the fatigue life required can be achieved.

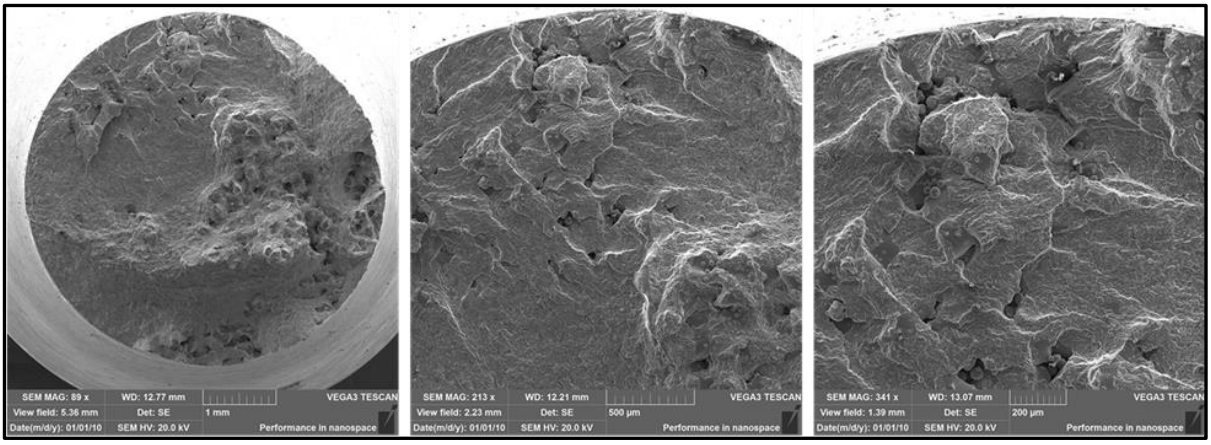

Figure 8: Tray #3 Specimen (HIP) of Low-Fatigue-Life SEM/Fractographic failure analyses

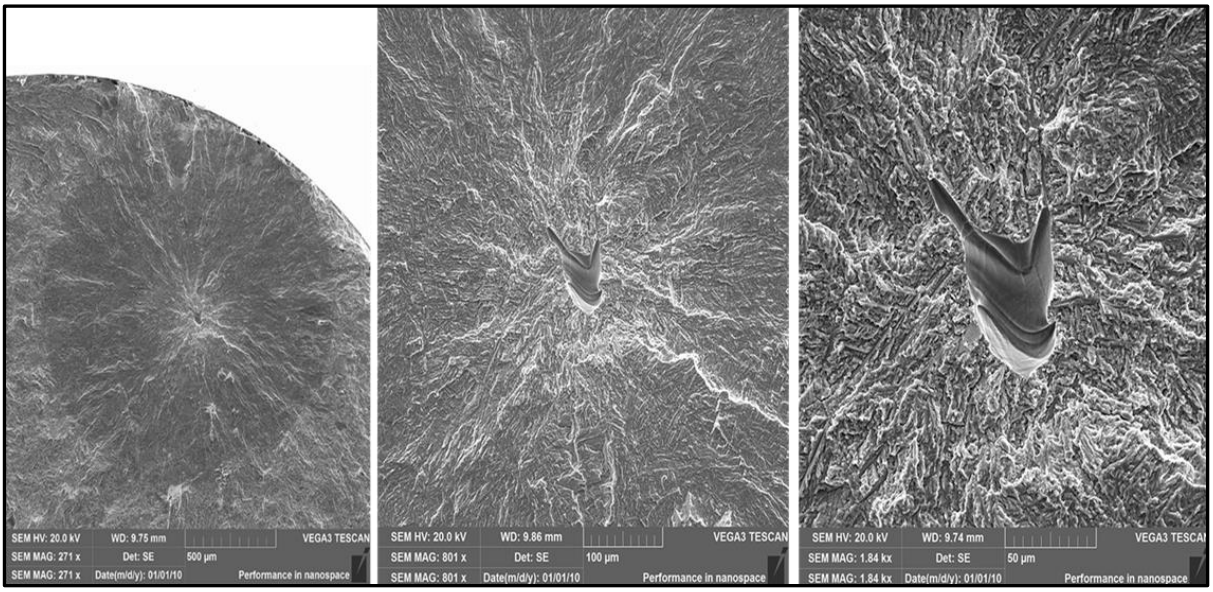

Figure 9: Tray #2 Specimen (No-HIP) of High-Fatigue-Life SEM/Fractographic failure analyses.

CONCLUSIONS

Serial production quality control should detect the AM technology inherent defect types of: Pores (Local Voids), Lack of Fusion Surfaces and Inclusions (Contaminations) that may compromise required fatigue strength (note: residual-stress type of defects should be eliminated via Heat-Treatment applied). This study characterized AM Ti-6AL-4V defects for quality control acceptance criteria. Further studies are needed for detailed rejection criteria, to enable qualification control to ensure meet fatigue strength requirements for airframe load carrier structural items.

Based on [3] and in accordance with this study findings (dealing with the defects specified above), the following Ti-6AL-4V AM relations to fatigue-strength-quality-measure can be said:

- Strong indicator for AM quality-measure –
  - Life results for fatigue crack initiation.
  - Defects findings per: defect type, size and its distance from surface.
- Not an indicator for AM quality-measure –
  - Life results for fatigue crack growth.
  - Material density correspondence to Forges/Plates Ti-6AL-4V, do not guarantee good compliance to fatigue-strength requirements (compliance relates to specific combinations of defect type, size and distance to surface). Note: low density most likely guarantees not meet fatigue requirements.

According to combined information gained at this study from the fatigue (crack initiation) test results, Micro-CT inspections and SEM/Fractographic failure analyses, the following defect characteristics for pores (local voids), inclusions (contaminations) and lack of fusion surfaces, can be concluded:

- Surface (and very near surface) – Any type of defect and of any size, will cause early fatigue cracking, that will prevent to meet the fatigue requirements for Airframe structures (as a defect is being closer to surface, smaller defect sizes will become critical for fatigue strength).
- Internal (volumetric) defects – Defects that their size is up-to 120μm and their distance from surface is more than 10 times their size, will not cause early fatigue cracking, and will allow to meet the fatigue requirements for Airframe structures. Further investigations are needed to extend that criterion to more detailed criteria, for having functions of defect size per distance from surface, to each of the above specified defect type (pore, inclusion and lack of fusion surface).

Location on the printing tray may influence the printing quality, as it was shown that locations near the chamber's Argon-Gas Inlet/Outlet were related to low elongation and low fatigue life results, as these locations are more prone to higher inclusion (contamination) density ambience, inducing such defects.

REFERENCES

[1] Part 25 of the USA Federal Aviation Regulations (FAR), 14 CFR § 25.571 - Damage-tolerance and fatigue evaluation of structure.
[2] Non-Destructive Techniques and Technologies for Qualification of Additive Manufactured Parts and Processes: A Literature Review, Report: DRDC-RDDC-2015-C035, March 2015, Defence Research and Development Canada – Atlantic Research Centre (prepared by: Dr. Bree M. Sharratt, Sharratt Research & Consulting Inc.).
[3] S. Leuders, M. Thöne, A. Riemer, T. Niendorf, T. Tröster, H.A. Richard, H.J. Maier (2012) On the mechanical behavior of titanium alloy TiAl6V4 manufactured by selective laser melting: Fatigue resistance and crack growth performance, International Journal of Fatigue, Elsevier.
[4] ASTM E8, Standard Test Methods for Tension Testing of Metallic Materials.
[5] ASTM E466-15, Standard Practice for Conducting Force Controlled Constant Amplitude Axial Fatigue Tests of Metallic Materials.
[6] ASTM E647-15, Standard Test Method for Measurement of Fatigue Crack Growth Rates.
[7] AATiD CONSORTIUM – Development of Advanced Technologies for 3D Printing of titanium Aero-structures, Rev. 2.0, Israel Innovation Authority, "The effect of process parameter modification on the final part surface roughness and porosity level", p. 270.
[8] MMPDS Handbook - Metallic Materials Properties Development and Standardization (MMPDS): The primary source of statistically-based design allowable properties for metallic materials and fasteners used for commercially and military aerospace applications (recognized by certifying agencies within their limitations: including FAA, DoD and NASA).
[9] NASGRO - Fracture Mechanics and Fatigue Crack Growth Analysis Software; Version 10.0.
[10] Kevin D. Rekedal, Captain, Investigation of the High-Cycle Fatigue Life of Selective Laser melted and Hot Isostatically Pressed TI-6AL-4V, USAF, AFIT-ENY-MS-15-M-212, AIR FORCE INSTITUTE OF TECHNOLOGY, Wright-Patterson Air Force Base, Ohio.